

## Spherical NiO-C composite for anode material of lithium ion batteries

X.H. Huang, J.P. Tu<sup>\*</sup>, C.Q. Zhang, X.T. Chen, Y.F. Yuan, H.M. Wu

*Department of Materials Science and Engineering, Zhejiang University, Hangzhou 310027, China*

Received 24 August 2006; received in revised form 7 November 2006; accepted 26 November 2006

Available online 9 January 2007

### Abstract

Spherical NiO-C composite was prepared by dispersing spherical NiO in glucose solution and subsequent carbonization under hydrothermal conditions at 180 °C. The microstructure and morphology of the NiO-C and NiO powders were characterized by means of X-ray diffraction (XRD) and scanning electron microscopy (SEM). The electrochemical properties of the electrodes were measured by galvanostatic charge–discharge tests, cyclic voltammetric analysis (CV), and electrochemical impedance spectroscopy (EIS). SEM images showed that the amorphous carbon not only coated on the surface but also filled the inner pores of the NiO spheres. Electrochemical tests showed that the NiO-C composite exhibited higher initial coulombic efficiency (66.6%) than NiO (56.4%), and better cycling performances. The improvement of these properties is attributed to the carbon, as it can reduce the specific surface area of porous sphere, and enhance the conductivity of porous NiO.

© 2007 Published by Elsevier Ltd.

*Keywords:* NiO; NiO-C composite; Anode material; Lithium ion battery

### 1. Introduction

Transition-metal oxides such as CoO, Co<sub>3</sub>O<sub>4</sub>, NiO, Cu<sub>2</sub>O, CuO, FeO, Fe<sub>2</sub>O<sub>3</sub>, and MnO have attracted much attention. These oxides offer a promising carbon alternative to negative-electrode materials in lithium ion batteries [1–13], which is attributed to their high specific capacity and good cycling performance. A mechanism different from the classical Li insertion/deinsertion in carbonaceous compounds or Li-alloying processes in alloy electrode is proposed, which can be written as:  $M_xO_y + 2y Li \leftrightarrow y Li_2O + xM$  [2]. Solid electrolyte interface (SEI) will also be formed during the discharge, but it will partially decompose during the subsequent charge process, which is attributed to the catalytic activity of metallic nanoparticles [11]. The partially reversible formation/decomposition of SEI film will lead to an extra capacity.

NiO has a theoretic capacity of 718 mAh g<sup>-1</sup> when it is used as anode material for lithium ion batteries. However, the initial coulombic efficiency and cycling performance of NiO are worse than those of other transition metal oxides such as CoO,

CuO, and Cu<sub>2</sub>O [2,3]. The electrochemical properties of metal oxide electrodes are related to various factors, such as the specific surface areas, the large change in volume and the serious aggregation of active particles during charge–discharge. Spherical particle, as it is known, with the smallest specific surface area which results in less of SEI film during the discharge, can increase the initial coulombic efficiency. It was reported that the cycling performance of Sn [14,15], SnO<sub>2</sub> [16,17], Si [18,19], TiO<sub>2</sub> [20] had been significantly enhanced by forming composite with carbon. The carbon can act as a barrier to suppress the aggregation of active particles and thus increase their structure stability during cycling [14,16,20], and also act as a buffering matrix to relax the expansion that occurred within the electrode upon lithiation/delithiation process [18,19]. Furthermore, the carbon has a high electronic conductivity and it can improve the conductance of the active materials [17]. Therefore, a synthesis of composite with carbon is an effective way to improve the electrochemical performance of electrodes. In this present work, spherical NiO-C composite was prepared by dispersing spherical NiO in glucose solution and subsequent carbonization under hydrothermal conditions at 180 °C. The electrochemical properties of the NiO-C composite were investigated by galvanostatic discharge–charge test, cyclic voltammetric analysis (CV), and electrochemical impedance spectroscopy (EIS).

<sup>\*</sup> Corresponding author. Tel.: +86 571 87952573; fax: +86 571 87952856.  
E-mail address: [tujp@cmsce.zju.edu.cn](mailto:tujp@cmsce.zju.edu.cn) (J.P. Tu).

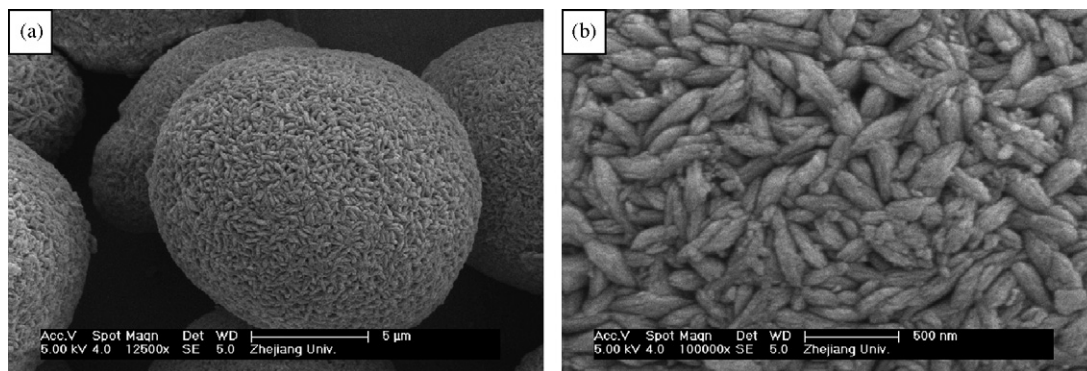


Fig. 1. SEM images of the spherical  $\text{Ni}(\text{OH})_2$  precursor: (a) the morphology of a whole sphere and (b) the magnified image of the surface of the sphere.

## 2. Experimental

Commercial spherical  $\beta\text{-Ni}(\text{OH})_2$  (about 10  $\mu\text{m}$  in diameter) was used as the precursor. Spherical NiO was obtained by calcining  $\text{Ni}(\text{OH})_2$  under flowing oxygen in a quartz tube furnace at 350  $^\circ\text{C}$  for 30 min. The NiO-C composite was prepared as follows. Glucose (3.17 g) was dissolved in deionized water (80 mL) until a clear solution was observed. Then the as-prepared NiO (2.88 g) was dispersed in the resulting solution. It was reported that glucose would be carbonized under hydrothermal conditions at 180  $^\circ\text{C}$  [15,21]. In this work, the mixture was placed in a flask under magnetic stirring for 2 days, and then removed to a 120 mL teflon-sealed autoclave filled with Ar maintained at 180  $^\circ\text{C}$  for 3 h. The products were centrifuged and washed with deionized water and ethanol for three times, respectively, and were dried in vacuum at 160  $^\circ\text{C}$  for 24 h. The structure and morphology of these products were characterized by X-ray diffraction (XRD, Rigaku D/max-rA; Cu  $\text{K}\alpha$  radiation) and scanning electron microscopy (SEM, FEI SIRION, equipped with EDX).

The working electrodes were prepared by a slurry procedure. The slurry consisted of 75 wt.% active materials, 15 wt.% acetylene black and 10 wt.% polyvinylidene fluoride (PVDF) dissolved in *N*-methyl pyrrolidinone (NMP), and was coated on a copper foam (1.3 cm in diameter) acted as current collector. The foam was pressed under a pressure of 20 MPa after drying at 95  $^\circ\text{C}$  for 12 h in vacuum. Test cells were assembled in an argon-filled glove box using Li foil as counter electrode, polypropylene (PP) film (Celgard 2300) as separator. The electrolyte was 1 M  $\text{LiPF}_6$  in a 50:50 (w/w) mixture of ethylene carbonate (EC) and diethyl carbonate (DEC).

The galvanostatic charge–discharge tests were conducted on a PCPT-138-32D battery program-control test system with the cut-off voltages of 0.02 and 3.0 V (versus  $\text{Li}^+/\text{Li}$ ). Cyclic voltammetric measurements of the electrodes were performed on a CHI604B Electrochemical Workstation with a scan rate of 0.1  $\text{mV s}^{-1}$  between 0 and 3 V (versus  $\text{Li}^+/\text{Li}$ ). The electrochemical impedance spectroscopy of the electrode was also carried out on a CHI604B Electrochemical Workstation. Before the measurement, the electrodes were cycled for 3 cycles, then discharged to 2.0 V and kept until the open-circuit voltage stabilized. The frequency of EIS ranged from 0.01 Hz to 100 kHz. A small ac signal of 5 mV in amplitude was used as the perturbation of the system throughout the tests.

## 3. Results and discussion

### 3.1. Characterization of materials

The morphology of  $\beta\text{-Ni}(\text{OH})_2$  precursor is shown in Fig. 1. It is clearly observed in the magnified image (Fig. 1b) that the surface of the  $\beta\text{-Ni}(\text{OH})_2$  microsphere is composed of spindle-like particles. XRD pattern of the precursor is shown in Fig. 2a and the diffraction peaks are corresponded with  $\beta\text{-Ni}(\text{OH})_2$ . After

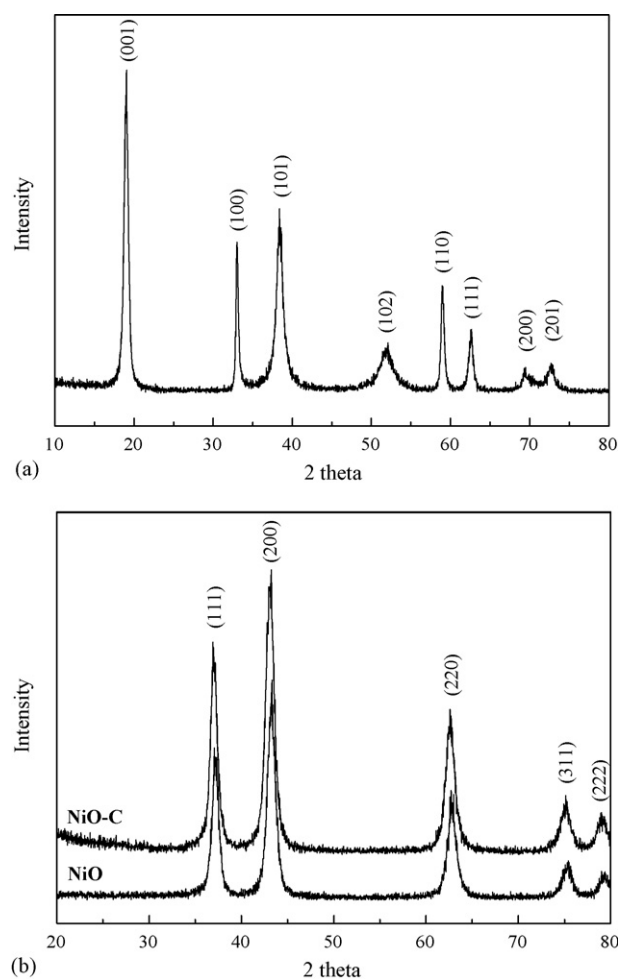


Fig. 2. XRD patterns of (a) the  $\text{Ni}(\text{OH})_2$  precursor and (b) the as-prepared spherical NiO and NiO-C composite.

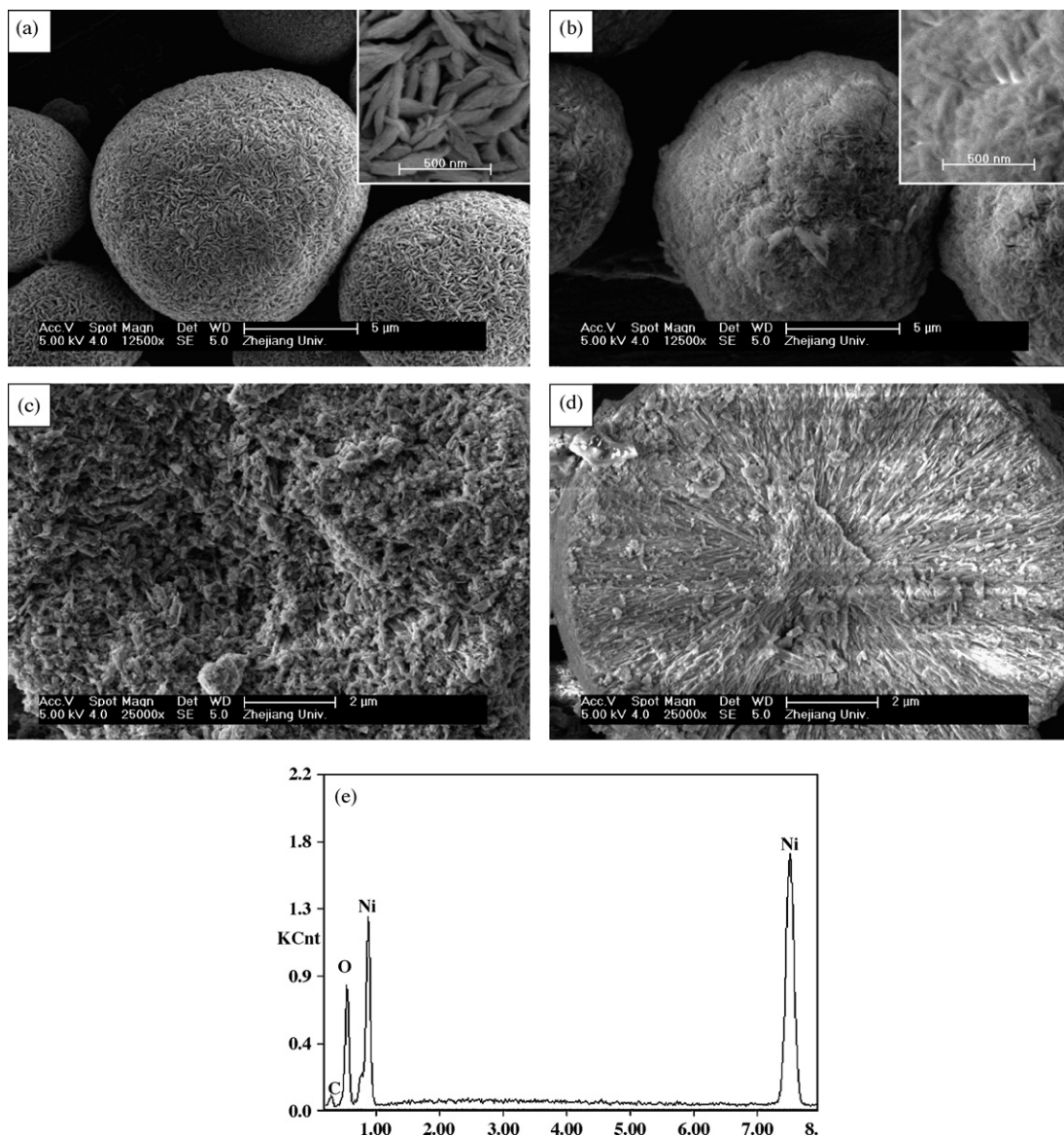


Fig. 3. SEM images of the as-prepared spherical (a) NiO and (b) NiO-C composite (insets: higher magnifications). The cross-sectional morphology of (c) a NiO sphere and (d) a NiO-C sphere. (e) EDX spectrum of the identical sample in (d).

the heat treatment at 350 °C for 30 min, the green Ni(OH)<sub>2</sub> powder turned to black. The XRD pattern of the as-calcined sample is shown in Fig. 2b. All the peaks can be assigned to cubic NiO and no impurities can be observed, indicating a complete decomposition of the Ni(OH)<sub>2</sub> precursor. A SEM image of the as-prepared NiO is given in Fig. 3a. The morphology of the microspheres was preserved after the decomposition of the Ni(OH)<sub>2</sub> precursor, but less compact spheres can be observed. The inset figure in Fig. 3a and the cross-sectional morphology of the NiO microspheres (Fig. 3c) indicate that these spheres have a porous structure.

The XRD pattern of the NiO-C composite is shown in Fig. 2b. Only peaks of cubic NiO can be observed, indicating that the carbon in the composite is amorphous. The surface of the NiO-C sphere is coated by a carbon layer (Fig. 3(b and d)), and no pores can be observed in the cross-section image of NiO-C spheres (Fig. 3d). All the original micropores in NiO spheres are filled with carbon. The content of carbon is

7.35 wt%, calculated according to the EDX result (Fig. 3e). Since the NiO microspheres are porous, the glucose solution can permeate into the inner pores of the NiO spheres. After carbonization in hydrothermal conditions, the carbon filled the pores. It can be also observed in Fig. 3d that there is a carbon layer coated on the surface of the spheres.

### 3.2. Electrochemical analysis

Fig. 4 shows the first galvanostatic discharge–charge curves for NiO and NiO-C electrodes measured between 0.02 and 3.0 V versus Li<sup>+</sup>/Li at a rate of 0.1–4C (1C = 718 mA g<sup>-1</sup>). Lower discharge capacity (849 mAh g<sup>-1</sup> at 0.5C) was observed for NiO-C at low rates (0.1, 0.5 and 1C) as compared to NiO (1025 mAh g<sup>-1</sup> at 0.5C). This would be due to its smaller surface area, which means less SEI. However, the capacity of NiO-C was remarkably higher at high rates (2 and 4C),

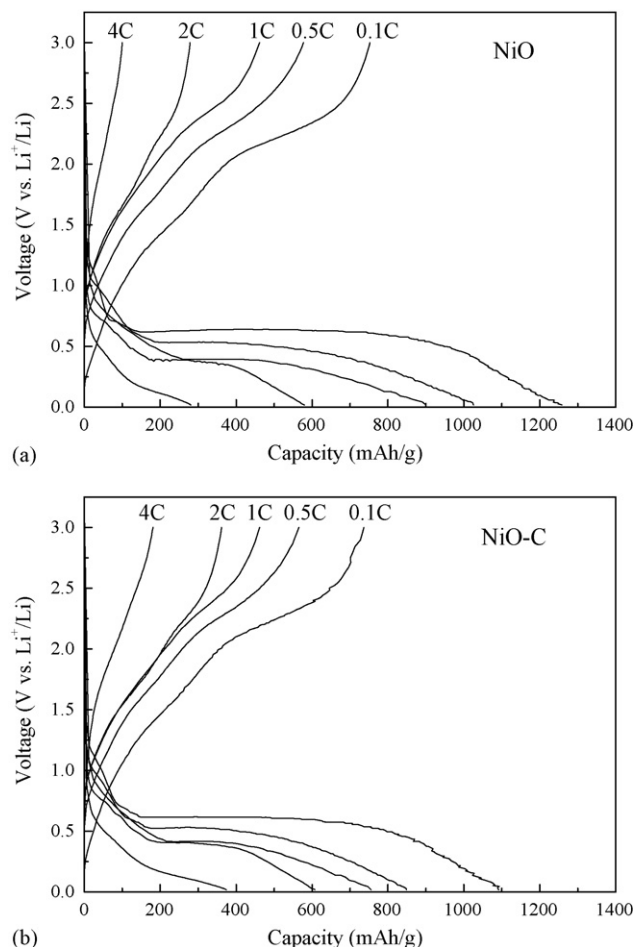


Fig. 4. Galvanostatic lithium-insertion/extraction curves of (a) NiO and (b) NiO-C at a rate of 0.1–4C ( $1C = 718 \text{ mA g}^{-1}$ ).

suggesting that the carbon facilitated the charge transfer at high charging–discharging rates. It can be seen that the potential hysteresis increased upon increasing the charging–discharging rate, but it was suppressed by the incorporation of carbon. It is calculated that the initial coulombic efficiency of NiO-C composite is higher than that of NiO at each charging–discharge rate. The initial coulombic efficiency of NiO-C composite is 66.6% at a rate of 0.5 C as compared to that for NiO (56.4%).

The cyclic voltammograms (CVs) of the NiO-C and NiO electrodes measured between 0 and 3 V (versus Li<sup>+</sup>/Li) at a scanning rate of  $0.1 \text{ mV s}^{-1}$  are shown in Fig. 5. The curves for both the electrodes show similar reduction and oxidation peaks. For the NiO, the reduction peak located at 0.89 V corresponds to the decomposition of NiO into Ni, and the formation of amorphous Li<sub>2</sub>O and the SEI. For the NiO-C composite, this peak shifts to 0.94 V. The two oxidation peaks located at about 1.51 and 2.35 V can be attributed to the decomposition of the SEI and Li<sub>2</sub>O, respectively [11,12]. For the NiO-C composite, these peaks shift to 1.47 and 2.32 V, respectively. The separation between the reduction and oxidation peaks ( $\Delta U$ ) of the NiO-C composite decreases in comparison with that of the NiO, demonstrative of weaker polarization and better reversibility. This is because the high electronic conductive carbon in the NiO spheres is beneficial for the diffusion of lithium ions. Similar

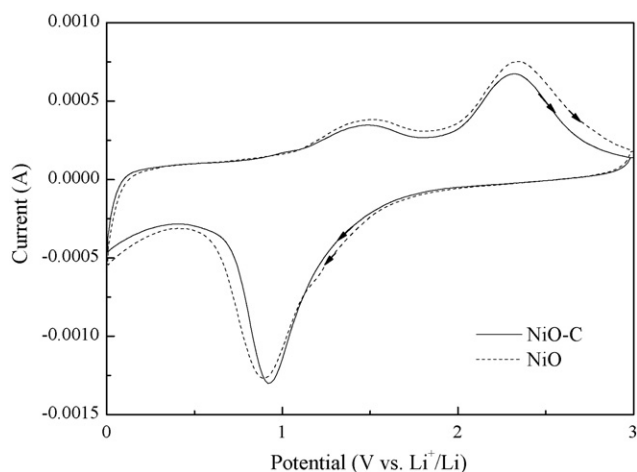


Fig. 5. Cyclic voltammograms of NiO and NiO-C electrodes measured between 0 and 3 V at the scan rate of  $0.1 \text{ mV s}^{-1}$ .

results were obtained for core/shell TiO<sub>2</sub>-C composite prepared by emulsion polymerization [20].

Fig. 6 shows the capacity retention properties of NiO-C and NiO electrodes at 0.5 C. Much better cycling performance was obtained for the NiO-C electrode. The specific capacity after 40 cycles for the NiO-C electrode is  $430 \text{ mAh g}^{-1}$ , much higher than that of the NiO electrode ( $200 \text{ mAh g}^{-1}$ ). There are several reasons for the poor cycling performance of NiO spheres. The SEI film is a poor conductive gel-like polymer, which contained LiF, Li<sub>2</sub>CO<sub>3</sub>, and lithium alkyl carbonate (ROCO<sub>2</sub>Li) [11], so more SEI will lead to poorer conductivity. The conductive carbon filled in the inner pores and coated on the shell of the spheres, it was able to keep the NiO particles in the spheres electrically connected and thus facilitate the charge transfer in the interface and in the inner of the spheres. Fig. 7 shows the electrochemical impedance spectrum (EIS) of the NiO and NiO-C electrodes. The high-frequency semicircle is attributed to SEI film and/or contact resistance, the semicircle in medium-frequency region is assigned to the charge-transfer impedance on electrode/electrolyte interface, and the inclined line at an

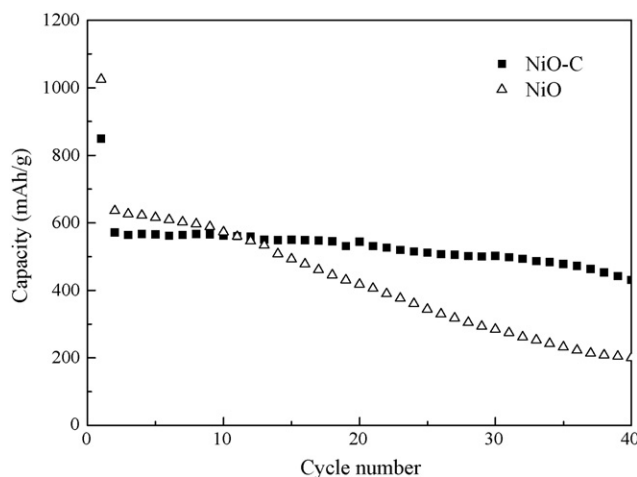


Fig. 6. Cyclic performances of the NiO and NiO-C electrodes cycled between 0.02 and 3.0 V at a current density of  $359 \text{ mA g}^{-1}$  (0.5C).

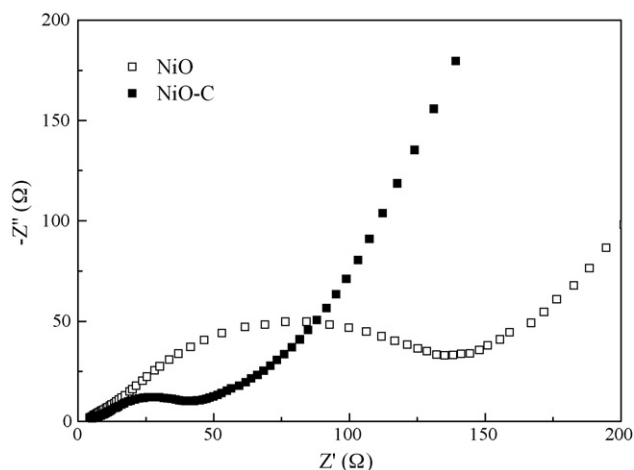


Fig. 7. AC impedance spectrum of NiO and NiO-C electrodes measured at the open potential of 2.0 V.

approximate  $45^\circ$  angle to the real axis corresponds to the lithium-diffusion process within electrodes [22]. It is obviously shown that the diameter of the semicircle in medium-frequency region for the NiO-C electrode is smaller than that of NiO, indicating lower charge-transfer impedances. This indicates that the addition of carbon had improved the electronic conductivity, and thus significantly improved the cycling performance.

#### 4. Conclusions

Spherical NiO-C composite was synthesized successfully by dispersing porous NiO microspheres in glucose solution and subsequent carbonization under hydrothermal conditions at  $180^\circ\text{C}$ . The carbon coated on the surface, and also filled in the inner pores of the NiO sphere. The NiO-C composite exhibited higher initial coulombic efficiency (66.6%) than the NiO (56.4%) at a charging–discharging rate of 0.5 C. Better cycling performance was also obtained for the NiO-C electrode. The specific capacity after 40 cycles for the NiO-C composite is  $430\text{ mAh g}^{-1}$ , higher than that of NiO ( $200\text{ mAh g}^{-1}$ ). These

improvements can be attributed to the conductive carbon and its combination with the pores. The carbon can reduce the specific surface area of the original porous sphere, keep the particles in the spheres electrically connected and thus improve the electrochemical performance of NiO.

#### References

- [1] J.-M. Tarascon, M. Armand, *Nature* 414 (2001) 359.
- [2] P. Poizot, S. Laruelle, S. Grugeon, L. Dupont, J.-M. Tarascon, *Nature* 407 (2000) 496.
- [3] P. Poizot, S. Laruelle, S. Grugeon, J.-M. Tarascon, *J. Electrochem. Soc.* 149 (2002) A1212.
- [4] K.T. Nam, D.-W. Kim, P.J. Yoo, C.-Y. Chiang, N. Meethong, P.T. Hammond, Y.-M. Chiang, A.M. Belcher, *Science* 312 (2006) 885.
- [5] W.Y. Li, L.N. Xu, J. Chen, *Adv. Funct. Mater.* 15 (2005) 851.
- [6] D. Larcher, G. Sudant, J.-B. Leriche, Y. Chabre, J.-M. Tarascon, *J. Electrochem. Soc.* 149 (2002) A234.
- [7] Y.M. Kang, M.S. Song, J.H. Kim, H.S. Kim, M.S. Park, J.Y. Lee, H.K. Liu, S.X. Dou, *Electrochim. Acta* 50 (2005) 3667.
- [8] Y. Wang, Z.W. Fu, Q.Z. Qin, *Thin Solid Films* 441 (2003) 19.
- [9] Y. Wang, Q.Z. Qin, *J. Electrochem. Soc.* 149 (2002) A873.
- [10] E. Hosono, S. Fujihara, I. Honma, H. Zhou, *Electrochem. Commun.* 8 (2006) 284.
- [11] S. Grugeon, S. Laruelle, R. Herrera-Urbina, L. Dupont, P. Poizot, J.-M. Tarascon, *J. Electrochem. Soc.* 148 (2001) A285.
- [12] A. Débart, L. Dupont, P. Poizot, J.-B. Leriche, J.M. Tarascon, *J. Electrochem. Soc.* 148 (2001) A1266.
- [13] J. Chen, L. Xu, W. Li, X. Gou, *Adv. Mater.* 17 (2005) 582.
- [14] K.T. Lee, Y.S. Jung, S.M. Oh, *J. Am. Chem. Soc.* 125 (2003) 5652.
- [15] M. Noh, Y. Kwon, H. Lee, J. Cho, Y. Kim, M.G. Kim, *Chem. Mater.* 17 (2005) 1926.
- [16] J. Fan, T. Wang, C. Yu, B. Tu, Z. Jiang, D. Zhao, *Adv. Mater.* 16 (2004) 1432.
- [17] Y. Wang, F. Su, J.Y. Lee, X.S. Zhao, *Chem. Mater.* 18 (2006) 1347.
- [18] G.X. Wang, J.H. Ahn, J. Yao, S. Bewlay, H.K. Liu, *Electrochem. Commun.* 6 (2004) 689.
- [19] Z.S. Wen, J. Yang, B.F. Wang, K. Wang, Y. Liu, *Electrochem. Commun.* 5 (2003) 165.
- [20] L.J. Fu, H. Liu, H.P. Zhang, C. Li, T. Zhang, Y.P. Wu, R. Holze, H.Q. Wu, *Electrochem. Commun.* 8 (2006) 1.
- [21] X. Sun, Y. Li, *Angew. Chem. Int. Ed.* 43 (2004) 597.
- [22] S. Yang, H. Song, X. Chen, *Electrochem. Commun.* 8 (2006) 137.